Distance-based Feature Extraction for Biometric Recognition of Millimeter Wave Body Images

Miriam Moreno-Moreno, Julian Fierrez
and Ruben Vera-Rodriguez
ATVS - Biometric Recognition Group
Universidad Autonoma de Madrid, EPS
C/ Francisco Tomas y Valiente, 11. 28049 Madrid. Spain
{*miriam.moreno, julian.fierrez, ruben.vera*}*@uam.es*

Josep Parron
AMS - Antenna and Microwave Systems Group
Universitat Autonoma de Barcelona
Campus de la UAB, 08193 Bellaterra, Barcelona, Spain
josep.parron@uab.es

***Abstract*—In this work a complete process of feature extraction for biometric recognition of Millimeter Wave body images is described. The scope of this work is to find a small set of distance-based features that can be used in body geometry authentication obtaining good error rates. This approach constitutes a feature-based alternative to the holistic recognition methods already proposed on the mentioned kind of images. The system is tested on a database comprising 1200 synthetic images at 94 GHz of the body of 50 individuals. The results prove that the use of a small number distance-based features provide good class separation.**

***Keywords*-millimeter wave images; 94 GHz; synthetic database; image processing; body geometry; distance-based features; feature extraction; feature selection.**

I. Introduction

Many of the biometric characteristics used to identify individuals, such as ear, face, hand, and gait, are extracted from images acquired by cameras working at visible frequencies of the electromagnetic spectrum. Such images are affected by, among others factors, lighting conditions and the body occlusion (e.g. clothing, make up, hair, etc.) In order to circumvent these limitations, researchers have proposed the use of images acquired at others spectral ranges: X-ray, infrared, millimeter (MMW) and submillimeter (SMW) waves [1]. The images captured beyond the visible spectrum overcome, to some extent, some of the mentioned limitations; furthermore, they are more robust to spoofing than other biometric images/traits. Among the spectral bands out of the visible spectrum, the millimeter waves (with frequency in the band of 30-300 GHz) present interesting properties that can be exploited in biometrics [2]: ability to pass through cloth and other occlusions, its health safety, its low intrusiveness, and the recent deployment and rapid progress of GHz-THz systems in screening applications. In spite of the previous advantages, to date, there is only one published research work that performs biometric recognition using that kind of images, using a holistic recognition approach [3]. This shortage of biometric recognition research based on MMW images is due, in part, to the lack of databases of images of people acquired at GHz. This lack is a consequence of: (i) the privacy concern these images present, and (ii) most of the imaging systems working at the MMW/SMW band are either in prototype form or not easily accesible for research.

In this contribution we proposed and study new methods for processing and feature extraction for MMW body images. First, a database composed by synthetic images of the body of 50 individuals is generated. After processing the images, different distance-based features are extracted from some landmarks related to the silhouette of the body. Finally, some experimental validations are performed to determine the most discriminative features, and its discrimination power.

The paper is structured as follows. The baseline corpus and the main characteristics of the used database are briefly presented in Sect. II. Sect. III describes all the steps followed to obtain the feature vector: image segmentation, boundary extraction, landmark generation and feature vector construction. The evaluation of the selected features is performed in Sect. IV, where a cualitative and a quantitative analysis is carried out. Conclusions are finally drawn in Sect. V together with future work.

Main Parameters	Corporal Measures	
Gender	Neck circ.	Waist circ.
Age	Height	Nape to waist
Tone	Upper arm circ.	Waist to hip
Weight	Upper arm length	Shoulder to Neck
Height	Lowerarm length	Upperleg height
	Wrist circ.	Lowerleg height
	Front chest dist.	Calf circ.
	Burst circ.	Angle circ.
	Underburst circ.	Thigh circ.
		Hips circ.

Table I
MAIN PARAMETERS AND BODY MEASURES FOR EACH SUBJECT.

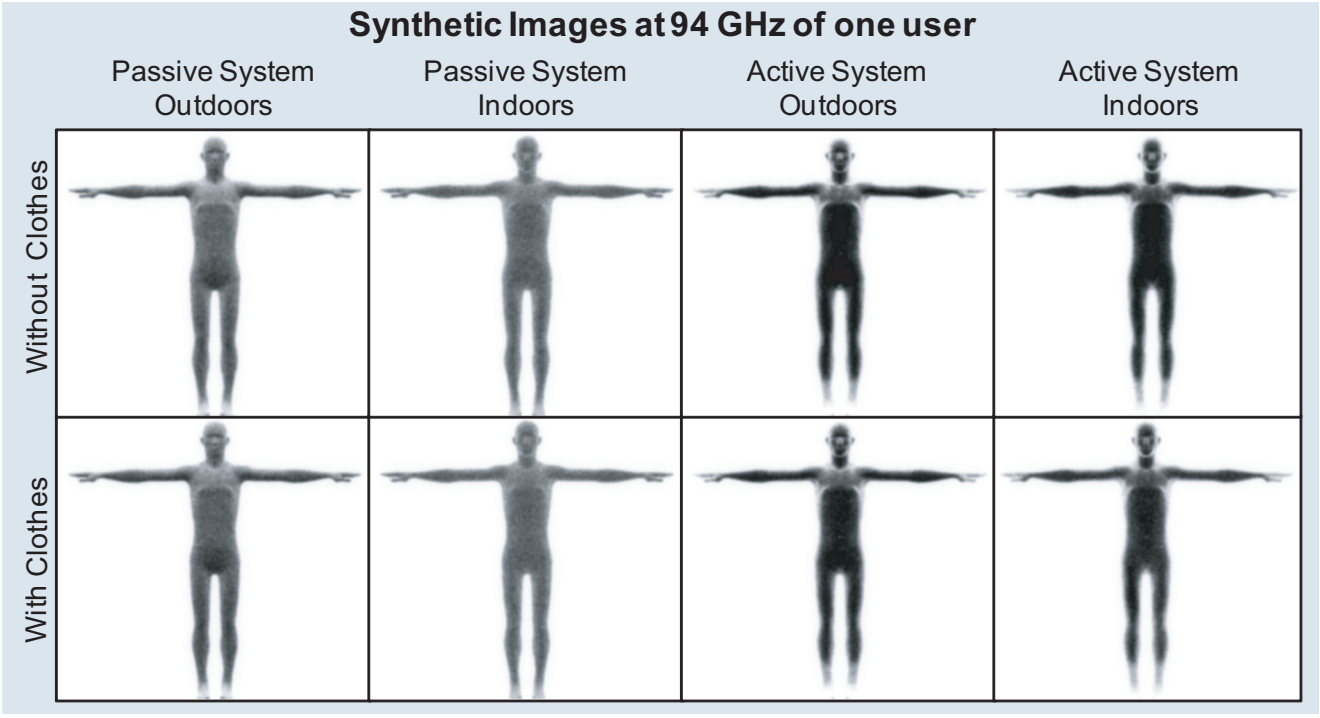

Figure 1. Synthetic images of one user simulated at 94 GHz with passive and active systems indoors and outdoors, and an orientation angle of the camera of 0 degrees.

II. BioGiga Database

The GHz-THz imaging technology is still in its infancy [4], therefore prices of the very few commercial imaging systems at that spectral band are still quite high. This fact together with the privacy problems the MMW images present, have caused the lack of public databases of MMW body images. That is the main reason why a synthetic database, called BioGiga, was generated in [5], with the objective of developing MMW-based biometric systems.

The baseline corpus of BioGiga consists of synthetic images at 94 GHz of the body of 50 individuals. The images are the result of simulations carried out on 3D-corporal models at two types of scenarios (outdoors, indoors) and with two kinds of imaging systems (passive and active). These corporal models were previously generated based on body measures taken from real subjects. The body measures considered are shown in Table I.

The database is gender balanced, consisting of 25 females and 25 males, with ages between 15 and 55 years old. For each user the database has four sets of images:

- Images simulated by a passive system outdoors.
- Images simulated by a passive system indoors.
- Images simulated by an active system outdoors.
- Images simulated by an active system indoors.

For each user and each of the previous sets the following data was generated:

- Images of the human 3D model with clothes and an angle formed by the camera of -10, 0 and +10 degrees.
- Images of the human 3D model without clothes and an angle formed by the camera of -10, 0 and +10 degrees.

According to what is stated above, for each user the database has $4\times2\times3=24$ images at 94 GHz. Hence, the total number of images in BioGiga is $50\times24=1200$.

Fig. 1 shows some of the images of one subject.

In this contribution, only images obtained from passive imaging systems are considered. Consequently, two types of images are treated: passive outdoor and passive indoor.

III. Image Processing and Feature Extraction

In order to obtain a distance-based feature vector for every image, we proposed the following steps. They are depicted in Fig. 2.

A. Image Segmentation

The first step is to binarize the image, separating the background from the body. A characteristic of the images simulated by passive systems is the different grey level they present in different parts of the body. For instance the abdomen is much darker than the feet. This fact difficults the segmentation process. This problem was overcome performing the segmentation in two steps:

- Border detection.
- Morphological operations.

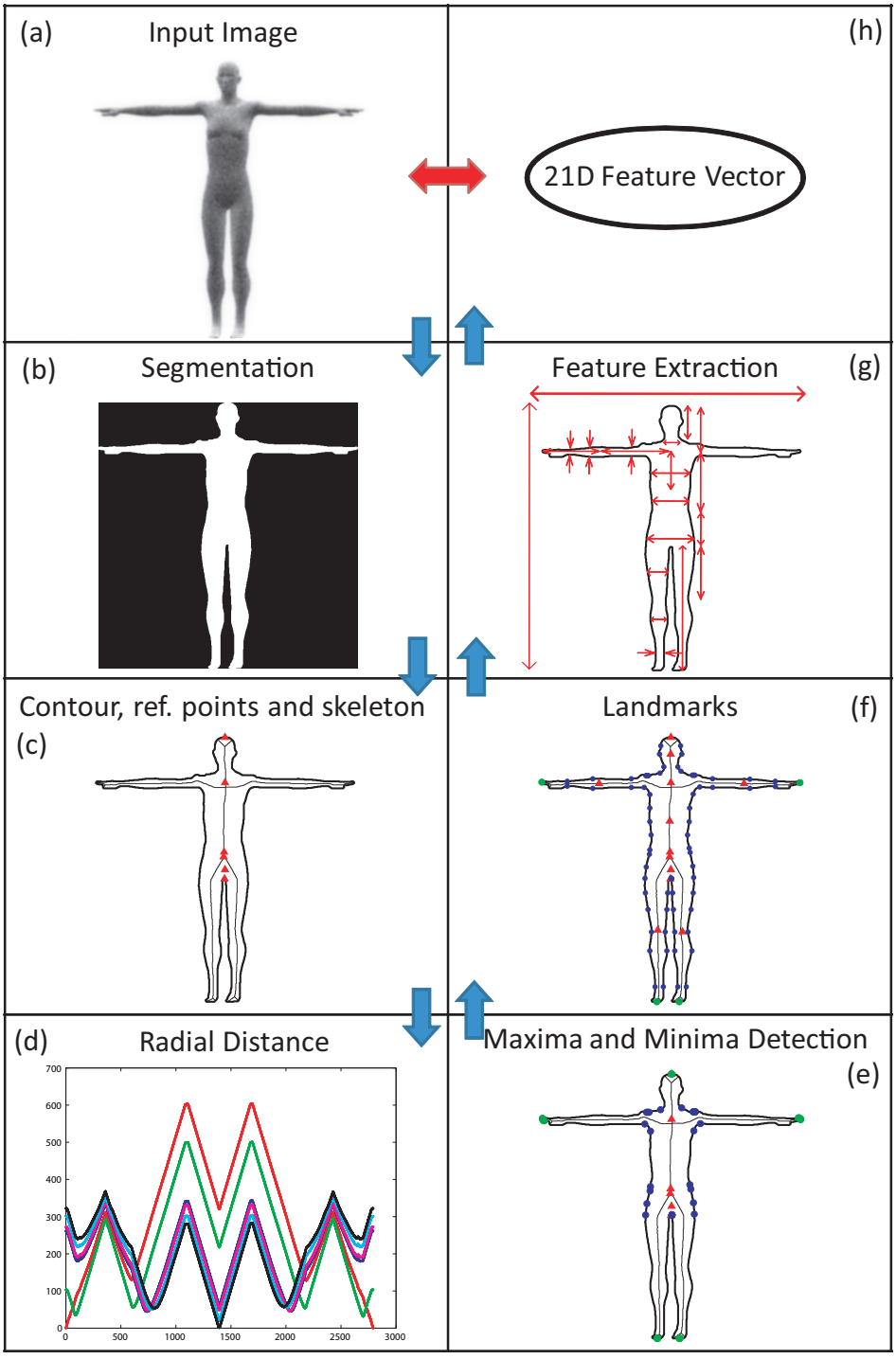

Figure 2. Main steps followed in our system to extract features. Original image (of a subject with clothing and a camera angle of -10 degrees) (a), segmented image (b), contour, reference points and skeleton (c), radial distance from each reference point to the contour (one curve per reference point) (d), addition of points with maximum and minimum distance from the reference points (e), all landmarks (f), distances used to form the feature vector (g) and the 21D feature vector (h).

A Canny border detector (whose parameters are previously tuned) is first applied to the image. After that, various morphological operations are conducted on the resulting border image. These morphological operations consists of closing operations with different structural elements in different areas of the image (head, arms, from arms to calf, and feet). Finally another set of morphological closing removes spurious irregularities.

An example image after this segmentation step is shown in Fig. 2(b)

B. Boundary Extraction

Once the input image is properly segmented, only the largest connected component is considered, assuming that it is the body. Then, the body boundary is extracted. After that, the middle point of the top of the head is detected. This point is fixed to be the first point of the extracted contour. The rest of the coordinates of the boundary are ordered in a clockwise direction. In addition to the boundary of the body, a basic skeleton of the body is obtained by means of morphological operations.

C. Landmark Generation

Six different reference points are first considered: (i) middle point of the top of the head, (ii) the crossing point of the arms line and the vertical line of the torso, (iii) the centroid of the body, (iv) the bifurcation of the skeleton in the abdomen area, (v) the central point of a bounding box including the whole body, and (vi) the pubis. An example image obtained after boundary extraction and the reference points detection is depicted in Fig. 2(c).

For each reference point, the Euclidean distance between the reference point and every point of the boundary is computed. Therefore, a one-dimensional function, showing the radial distance, is obtained for each reference point. An example of the six resulting radial distance functions is shown in Fig. 2(d). Every function is examined to find local maxima and minima. Maxima of the curve correspond to the head, hands, and feet outer points, while the minima correspond to points near the neck, shoulders, axilla, wrist and hips, depending on the considered reference point. Fig. 2(e) shows an example boundary together with the reference points and the maximum and minimum distance points.

In order to have enough geometric measures of the body, several extra points are detected inside the area of the body and in its boundary. To summarize, the following points are detected (see Fig. 2(f)):

- The centroid of some parts of the body: head, arms, torso and legs.
- Some points located at the boundary of the above mentioned body parts (for example in case of the torso, the points of the torso boundary located at three different heights are detected: at one quarter, at a half and at three quarters of the torso height.)

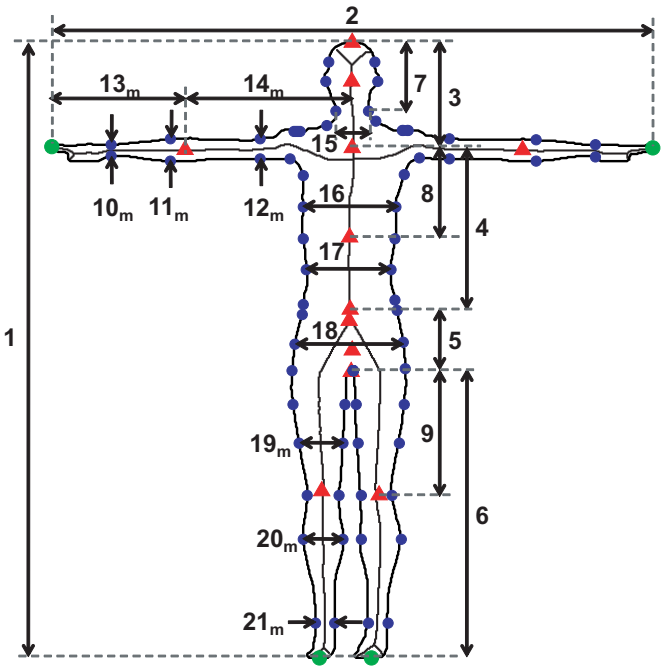

Figure 3. Body boundary, landmarks and distances extracted among them of the subjects and conditions of Fig. 2. These distances form the 21D feature vector. The number next to every distance is the component number in the feature vector. The ones whose number component appears with a subindex m are calculated as the average of that distance and the analog one of the right extremity. Red triangles represent the reference points and centroids of head, arms, legs and torso. Blue circles represent landmarks on the silhouette of the body (some of the them have minimum distance to the reference points). Green circles represent landmarks with maximum distance from the reference points.

D. Feature Generation

Once all the landmarks are obtained, the Euclidean distance between some of them is calculated. Specifically, 21 distances are obtained, which constitutes the feature vector. Fig. 2(g) and Fig. 3 show the considered distances. In Fig. 3, next to every distance there is a number that represents the component number in the feature vector (e.g. the height is the first component of the feature vector, it is feature number 1).

IV. Experimental Validation

In the following analysis only images simulated by a passive system indoors and outdoors are considered. The graphical results are shown exclusively for passive indoors images, for outdoors the results are quite similar. The same analysis for images simulated by active systems (indoors and outdoors) will be part of future work, in which a different image segmentation should be followed due to clearly visible differences between the images simulated by passive and active systems (e.g. the last ones present higher contrast).

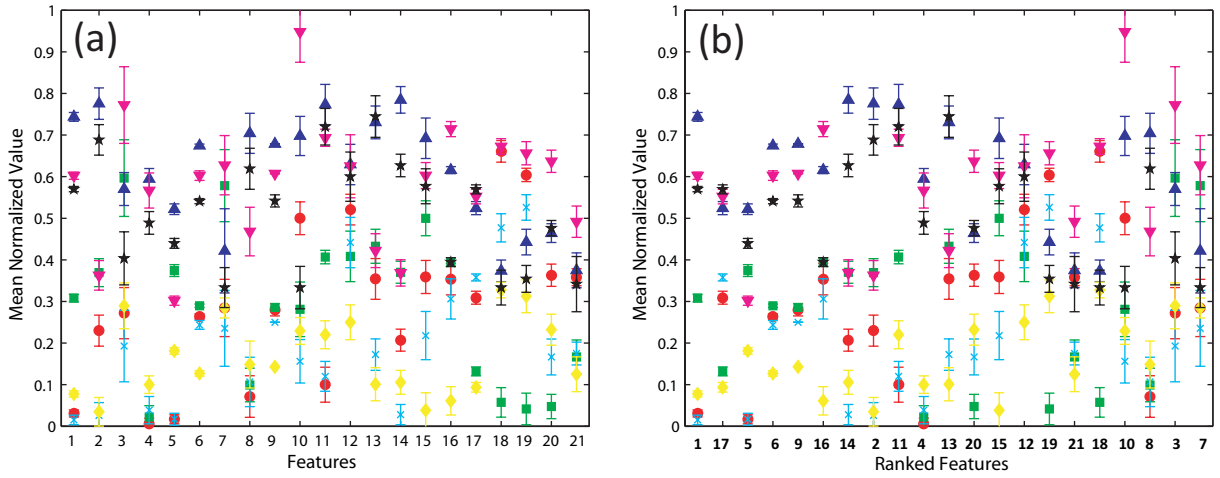

Figure 4. Mean normalized value of the feature vector of 7 randomly selected users. Each user vector has a different color and symbol.

A. *Evaluation of Features*

Fig. 4(a) represents the mean value and the standard deviation (as an error bar) of each normalized component (distance) of the feature vector, for seven subjects (a different color and symbol for each subject) randomly selected from the 50 available. As it can be seen, some component values are quite different from one subject to another, while others are more similar. On the other hand, the error bars overlap in some cases. To determine the most discriminative features, the components of the feature vector are ranked in descending order of degree of discrimination. For this purpose two magnitudes are calculated:

- **The average separation** between the mean values of each component from all subjects.
- **The overlap** between the error bars of the same component among all subjects.

The most discriminative feature will be the one with the largest average separation and the lowest overlap among different users. Hence, the features are ranked in descending order of the value of the quotient $average\_separation/overlap$. Fig. 4(b) shows the feature vector for the same seven subjects of Fig. 4(a) once its components have been ordered. Although the Fig. 4(b) shows the feature vector for 7 users, the ranking was conducted taking into account the vectors from all the 50 subjects. It can be seen the decreasing separation between mean values and the increasing overlap. The initial feature number (the same one as the one in Fig. 3) is written below the x axis with bold numbers. It is worth noting that the three most discriminative components (the three first ones in Fig. 4(b)) are: (i) the 1^{st} (height), (ii) the 17^{th} (waist width aprox.) and (iii) the 5^{th} (the distance between the centroid of the body and the pubis). The least discriminative one corresponds to feature 7^{th} (height of the head). Furthermore, these four features (three best ones and the worst one) obtained for images simulated by passive systems outdoors are the same ones when using images simulated indoors. It is not surprising that the height of the head is the least discriminating feature due to the process followed to obtain the 3D-body model from the body measures of real subjects. The head height was not considered, so all the models present approximately the same head height in their 3D body model used to simulate MMW images.

B. *Discrimination Power Analysis*

With the purpose of better assessing the discrimination power of the features, they are plotted in 2D graphs in Fig. 5:

- Fig. 5(a) plots the second PCA component vs the first PCA component of the 300 feature vectors (6 per user), having used all the 21D vectors to obtain the PCA transformation matrix.
- Fig. 5(b) plots the second most discriminative feaure (waist width aprox.) vs the most discriminative one (the height).

In both plots every user has its own color and symbol, so every user should be represented by a cluster of symbols with the same color and shape. In both cases, Fig. 5(a) and Fig. 5(b), it is patent that the clusters are clearly separated. Only in some regions of the 2D subspace some clusters overlap. This fact proves that the selected features are discriminative. Comparing both plots, it seems that the clusters in Fig. 5(b) are smaller and more separated among them than in Fig. 5(a). This reveals that even with only two features (height and waist width) it would be possible to distinguish different users. It must be noted that this analysis validates the proposed features but does not estimate their practical recognition capabilities. For doing so classification experiments should be performed, which will be conducted in future work.

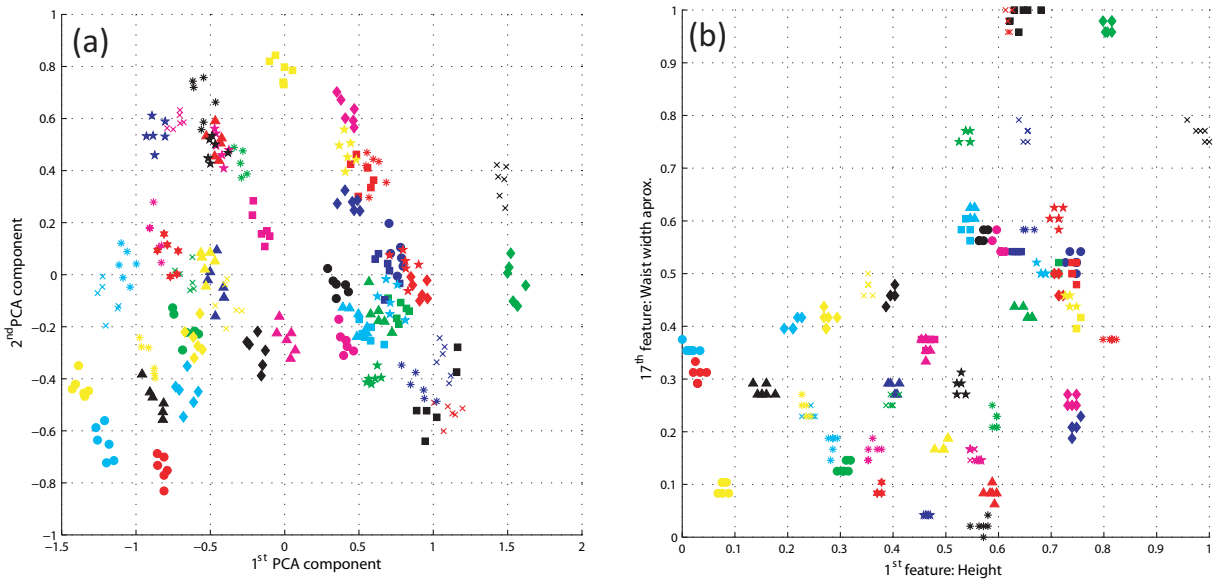

Figure 5. Bidimensional representation of the discrimination power of the extracted features. Second PCA component vs the first PCA component of the 300 feature vectors (6 per user) (a). Second most discriminative feature (waist width aprox.) vs the most discriminative one (the height) (b). In both plots every user has its own color and symbol.

V. Conclusions

A new feature extraction method for MMW images has been proposed. This method is based on the detection of relevant points of the body followed by the measure of 21 distances among them. These distances form the feature vector of every image. After an analysis of the selected features (using PCA and ordering them according to their individual discrimination degree), it has been proven that they have enough discrimination power to distinguish different users. Furthermore, even with only the two most discriminating distances, the users seem to be well classified.

The limitations of this work are related to the special characteristics of the database used. The BioGiga database is composed by images of only 50 users, besides, it consists of synthetic images. These two facts make the corpus limited when compared to the real data found in practice. However, the synthetic images are very similar to the ones really captured at 94 GHz (compare Fig. 1 with the images in [3].) Also, the synthetic images used are based on real measures from people. Therefore, the proposed features can be directly applied and are useful for practical MMW images.

Finally, the presented system should be completed with a classification stage. This will allow us to perform identification and/or verification experiments and to quantify the error rate using the 21D feature vectors or vectors with less components. A complete biometric system based on the proposed features for MMW images could be applied in the near future at airport security checkpoints and another screening scenarios.

Acknowledgment

This work has been partially supported by projects Bio-Challenge (TEC2009-11186), Contexts (S2009/TIC-1485), TeraSense (CSD2008-00068) and "Catedra UAM-Telefonica".

References

[1] M. Moreno-Moreno, J. Fierrez, and J. Ortega-Garcia, "Biometrics Beyond the Visible Spectrum: Imaging Technologies and Applications," in *Proceedings of BioID-Multicomm 2009*, ser. LNCS, vol. 5707. Springer, September 2009, pp. 154–161.

[2] ——, "Millimeter- and Submillimeter-Wave Imaging Technologies for Biometric Purposes," in *Proceedings of XXIV Simposium Nacional de Union Cientifica Internacional de Radio*, September 2009.

[3] B. Alefs, R. den Hollander, F. Nennie, E. van der Houwen, M. Bruijn, W. van der Mark, and J. Noordam, "Thorax biometrics from Millimetre-Wave images," *Pattern Recognition Letters*, vol. 31, no. 15, pp. 2357–2363, 2010.

[4] J. Mait *et al.*, "94-GHz Imager With Extended Depth of Field," *IEEE Transactions on Antennas and Propagation*, vol. 57, no. 6, pp. 1713–1719, June 2009.

[5] M. Moreno-Moreno, J. Fierrez, P. Tome, R. Vera-Rodriguez, J. Parron, and J. Ortega-Garcia, "BioGiga: Base de datos de imagenes sinteticas de personas a 94 GHz con fines biometricos," in *Proceedings of XXVI Simposium Nacional de Union Cientifica Internacional de Radio*, September 2011.